Polarization Oscillations in Birefringent Emitter-Cavity Systems

Thomas D. Barrett, Oliver Barter, Dustin Stuart, Ben Yuen, and Axel Kuhn*
University of Oxford, Clarendon Laboratory, Parks Road, Oxford OX1 3PU, United Kingdom

(Received 29 November 2018; published 1 March 2019; corrected 9 May 2019)

We present the effects of resonator birefringence on the cavity-enhanced interfacing of quantum states of light and matter, including the first observation of single photons with a time-dependent polarization state that evolves within their coherence time. A theoretical model is introduced and experimentally verified by the modified polarization of temporally long single photons emitted from a ^{87}Rb atom coupled to a high-finesse optical cavity by a vacuum-stimulated Raman adiabatic passage process. Further theoretical investigation shows how a change in cavity birefringence can both impact the atom-cavity coupling and engender starkly different polarization behavior in the emitted photons. With polarization a key resource for encoding quantum states of light and modern micron-scale cavities particularly prone to birefringence, the consideration of these effects is vital to the faithful realization of efficient and coherent emitter-photon interfaces for distributed quantum networking and communications.

DOI: 10.1103/PhysRevLett.122.083602

Cavity quantum electrodynamics (CQED) allows for the nature of light and matter to be interrogated through the enhanced interaction of an emitter with the resonant modes of a cavity [1–3]. This allows these fundamental interactions to be leveraged for quantum technologies [4–8] and, consequently, realizing novel regimes in CQED has the potential to impact both foundational research and cutting-edge technological applications. Single photons are fundamental particles; they posses no deeper substructure; therefore it is tempting to consider their properties to be similarly immutable. However, CQED has shown photons to be a far richer resource, with a high degree of control demonstrated over the wave packets [9], frequency [10], polarization [11] and phase [12] of temporally long single photons. Here, we report the first observation of a single photon with a time-dependent polarization state that evolves along its wave packet. Moreover, this effect arises from a system increasingly prevalent in the pursuit of scalable quantum technologies.

The coherent interfacing of light and matter qubits lies at the heart of many quantum networking proposals [4–8], and the interaction of atomlike emitters with a single photonic mode of a resonator provides a platform for realizing this control. CQED is a vibrant field, with single atoms and ions particularly suitable candidates with which to realize network nodes and single-photon sources due to their inherently homogeneous nature. The *a priori* deterministic emission of single photons into well-defined quantum states has been realized in both atom-cavity [11,13–16] and ion-cavity systems [17]. Proof-of-principle quantum networking demonstrations have leveraged this control to, e.g., remotely entangle two atoms [18] and perform two-bit quantum gates [19–21]. Improving the efficiency and scalability of such systems ultimately requires increasing the strength and reliability of the emitter-cavity coupling, motivating the development of microcavity resonators with tightly confined optical modes. Micron-scale Fabry-Perot cavities, such as those formed between laser-ablated mirrors on the tips of optical fibers [22–24], provide open access to the mode for ease of coupling and the trapping of single atoms [25] or ions [26–28]. Moreover, work with Fabry-Perot microcavities has also demonstrated the enhanced coupling of light to molecules [29] and to a variety of solid-state emitters including nitrogen-vacancy centers [30,31], quantum dots [32–34], carbon nanotubes [35,36], and optomechanical devices [37–39]. However, on these length scales, the tightly curved mirrors are highly susceptible to birefringence [23,40–44]—a lifting of the degeneracy of the two polarization eigenmodes of the cavity—due to the elliptical curvature of the mirrors [45]. Polarization both strongly effects the interaction between light and atomic emitters, and is a potential basis for quantum information protocols [19,46], which has motivated the attempts to control this ellipticity-induced birefringece [42,44]. More generally, the effects of birefringence on light incident on cavities has been studied in ringdown spectroscopy [47,48], high-precision polarimeters [49], and even for cavity-stabilization proposals [50].

In this Letter we present the first investigation of the interaction of quantum states of light and matter within a

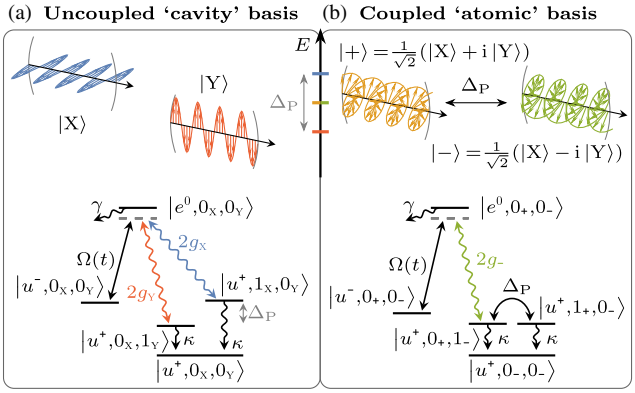

FIG. 1. Decomposition of cavity and Λ system into coupled and uncoupled polarization bases. The upper plots show how the linear polarization eigenmodes of a birefringent cavity can equivalently be considered as degenerate circularly polarized modes with an effective coupling between them. The lower plots equivalently illustrate a simple Λ-system coupling of circularly polarized transitions within an atom in both bases. The state notation is $|x^S, n_i, n_j\rangle$, with x^S denoting an atomic state x of spin S, and n_z the photon number in the cavity supporting mode $|Z\rangle$.

birefringent Fabry-Perot resonator. We use a single ^{87}Rb atom strongly coupled to a birefringent cavity and observe the dynamic change in polarization of the single photons emitted by a vacuum-stimulated Raman adiabatic passage (V-STIRAP) process [14,51,52]. Our experiment is uncommonly suited to this task, as our cavity exhibits non-negligible polarization-mode splitting despite being constructed with macroscopic mirror substrates—a technology that allows for the reliable coupling of atoms to the cavity.

We begin, however, with a simple theoretical description of a birefringent atom-cavity system.

We decompose the cavity into a pair of orthogonal polarization modes. These can be the nondegenerate polarization eigenmodes which independently couple to the atom, the so-called "cavity" basis, or the pair of polarizations which corresponds to the atomic transitions, the "atomic" basis. Figure 1(a) summarizes the system in the cavity basis for the extreme case where linearly polarized cavity eigenmodes couple circularly polarized atomic transitions. A photon is emitted into a superposition of the cavity eigenmodes, and these eigenmodes accumulate a phase difference at a rate Δ_P, the energy difference between them. This results in a time-dependent oscillation between any pair of orthogonal polarization states other than the cavity eigenmodes themselves. Viewed in the atomic basis [Fig. 1(b)], the photon is emitted into only one of the considered polarization states, with this oscillation then coupling the emitted state to its orthogonal counterpart.

Our approach can be formalized as an extension of the Jaynes-Cummings model, and these details can be found in the Supplemental Material [53].

At the heart of our experimental investigation is a cavity of non-negligible birefringence. The cavity is (339.289 ± 0.002) μm long with a measured finesse of $\mathcal{F} = 117800 \pm 200$. The mirrors have a 5 cm radius of curvature and a ∼1.5 mm diameter. Imbalanced mirror transmissions of ≤1.6 ppm and ∼40 ppm give a directional emission of the photons. Figure 2(b) shows a direct measurement of the cavity transmission from which we find two polarization eigenmodes, each with a line width of $\Delta\omega_{\mathrm{FWHM}}/2\pi = (3.543 \pm 0.006)$ MHz,

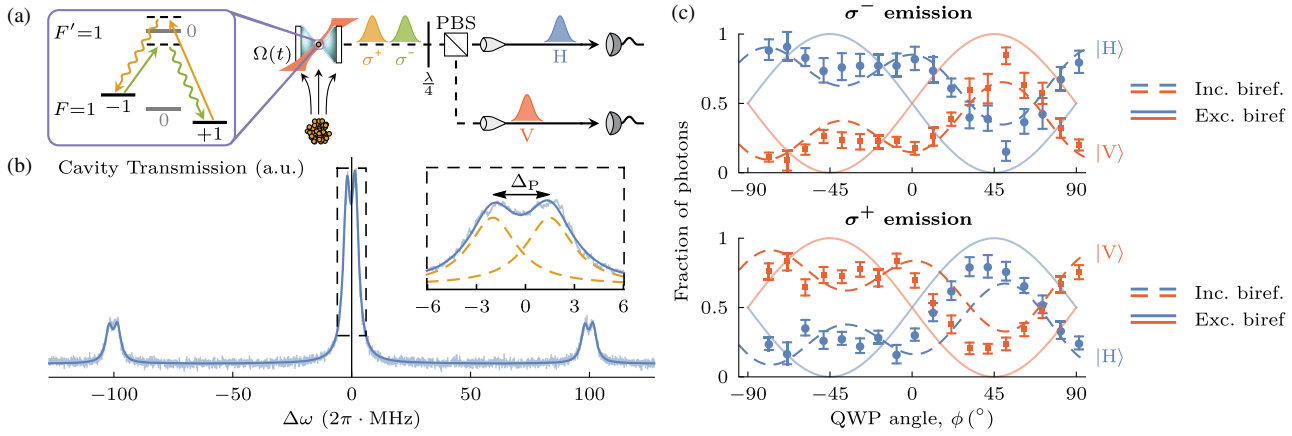

FIG. 2. Experimental summary. (a) Experimental setup for the production, routing, and detection of polarized single photons. The relevant couplings for each cavity-assisted Raman transition are distinguished by color. (b) The transmission of laser light through the cavity for direct characterization of cavity birefringence. The cavity length is scanned over resonance with an incident laser which has sidebands at ±100 MHz as a frequency reference. The double-peaked Lorentzian (an adequate line shape approximation for high-finesse cavities [62]) fit (solid blue) is comprised of the individual transmissions of the nondegenerate polarization eigenmodes (dashed orange). (c) Fractional routing of emitted photons as a function of the quarter-wave plate angle. The dashed and solid theory traces include and exclude the effects of cavity birefringence, respectively. The error bars in both plots are found from the $\pm\sqrt{N}$ uncertainty on N events exhibiting Poissonian counting statistics.

split by $\Delta_P/2\pi = (3.471 \pm 0.004)$ MHz. These eigenmodes are elliptically polarized, with $|X\rangle = 0.888|H\rangle + 0.459e^{-2.709i}|V\rangle$ and $|Y\rangle$ correspondingly orthogonal. In this work, the cavity is tuned such that the desired resonance is between these two eigenmodes [i.e., at $\Delta\omega = 0$ MHz in Fig. 2(b)]. The coupling parameters of the system are then $\{g, \kappa, \gamma\}/2\pi = \{4.77, 1.77, 3.03\}$ MHz, where κ is the cavity field decay rate and γ is the atomic amplitude decay rate, which places the experiment in the strong-coupling regime [61].

Each experimental cycle begins by loading ^{87}Rb atoms into a magneto-optical trap (MOT) ~8 mm below the cavity for ~500 ms. Atoms are then stochastically delivered into the cavity mode by an atomic fountain, which launches the MOT upwards at a velocity of ~1 ms^{-1}. The cloud is kept at a sufficiently low density such that we can consider only zero or one atom to be in the cavity at any one time. Polarized single photons are produced using a V-STIRAP process, summarized in Fig. 2(a), between the $|F = 1, m_F = \pm 1\rangle$ ground-state magnetic sublevels of the D_2 line [11,52]. An external magnetic field aligned along the cavity axis lifts the degeneracy of these sublevels by $2\pi \times 26$ MHz, allowing a pump laser and the cavity to form a Λ system with the $|F' = 1, m_{F'} = 0\rangle$ excited state. When the pump is detuned from the cavity resonance by $\pm 2\pi \times 26$ MHz, a Raman-resonant transition from $|m_F = \pm 1\rangle$ to $|m_F = \mp 1\rangle$ emits a $\sigma^{\pm}$ photon into the cavity. As the atoms traverse the cavity mode, 20 000 alternately detuned pump pulses—each with a $T = 333$-ns-long $\sin^4(t/T)$ intensity profile and a peak Rabi frequency of $\bar{\Omega}/2\pi = 10.0$ MHz [63]—attempt to produce a stream of alternately polarized photons at a repetition rate of ~1.5 MHz. A single atom takes ~60 μs to transit the mode, with waist $\omega_0 \sim 26.8$ μm, which corresponds to more than 100 photon production attempts. An atom can be considered to be effectively stationary—and thus the atom-cavity coupling unchanged—within the duration of a single pump pulse. The pump laser is linearly polarized and injected orthogonally to the cavity mode such that it decomposes into an equal superposition of σ^+ and σ^- light in the cavity basis. Single photons are detected by superconducting nanowire detectors [66]. The dark count rates range from 5 to 66 per hour across the battery of detectors, and are thus negligible. Every detection event is recorded at run-time with 81 ps precision by a time-to-digital converter [67]. A characterization of the produced photons—detailing their singular nature and coherence—can be found in the Supplemental Material [53].

We observe polarization states of photons emitted from the cavity that are significantly modified from those initially emitted by the atom. A polarization analyzer consisting of a quarter-wave plate and a polarizing beam splitter (PBS) split the photon stream into two paths prior to detection. Figure 2(c) shows the fractional routing of the photons as a function of the quarter-wave plate angle. The measured behavior coincides well with the model including birefringence effects (dashed traces) and is in disagreement with the simple prediction of the emission of circularly polarized photons (solid traces) [68], as would be expected in the case of negligible cavity birefringence.

The extreme length of the photons (333 ns, as determined by the duration of a pump pulse, in comparison to the <100 ps timing jitter of the detectors) allows us to examine how the polarization changes with time and so observe polarization oscillations within a single photon's wave packet. Figure 3 shows the time-resolved distribution of photon detections at each detector for three orientations of the routing quarter-wave plate. This corresponds to a measurement of the polarization state along the photon wave packet. The differing wave packet profiles measured at each detector show that the polarization state is changing along the photon length. This is a result of the birefringence-induced coupling between the two orthogonal polarization states onto which the photon is projected by our measurement. Only if we were measuring in the (uncoupled) cavity basis would the relative population of each polarization mode be unchanged along the photon length. This can again be contrasted to the expected behavior in the case of negligible cavity birefringence, where static photon polarizations would be emitted from the cavity. The photon counts at each detector would then be some constant fraction of the overall wave packet, regardless of the chosen measurement basis.

Having experimentally observed that cavity birefringence modifies the polarization of emitted photons, it is natural to consider some general limiting cases to further examine these effects. To isolate only the effects of birefringence, we return to the three-level system shown in Fig. 1 and consider the emission of σ^- photons. Realistic coupling parameters

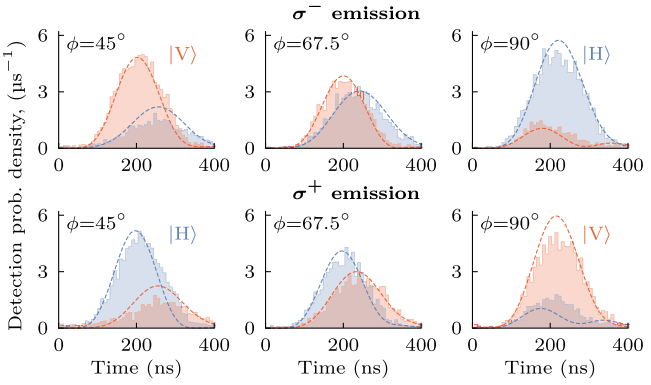

FIG. 3. Time-dependent polarization of the emitted photons. Measured data (solid traces, filled) overlaid with theoretical predictions (dashed traces) of the photon wave packets measured in various polarization bases using a quarter-wave plate at angle ϕ and a PBS. The blue and red wave packets correspond to detections in the different outputs of the PBS and so correspond to different polarizations. The measured data are presented as density histograms with bin widths of 8 ns.

are chosen, $\{g, \kappa, \gamma\}/2\pi = \{4, 2, 0\}$ MHz, disregarding spontaneous emission. While any physical system will be subject to this decay, in general it is a loss leading to an incoherent evolution which we ignore. If the cavity eigenmodes are aligned with the circularly polarized atomic basis, the system reduces to a simple three-level model with a single cavity coupling, and birefringence has no effect. Therefore, we consider the case of minimal overlap between the cavity and atomic bases—a "linear" cavity with $\{|X\rangle, |Y\rangle\} = \{|H\rangle, |V\rangle\}$.

Figure 4(a) summarizes the emissions with the birefringent cavity modes oppositely detuned from Raman resonance with the pump laser. With no birefringence ($\Delta_P/2\pi = 0$ MHz), the photon is emitted in the expected $|-\rangle$ mode with close to unity efficiency. As has already been seen in the measured output of our physical system, a birefringence that is comparable to the other coupling rates of the system (we take $\Delta_P/2\pi = 4$ MHz for our simulated system) results in a time-dependent polarization state of the emitted photon due to the coupling between the $|+\rangle$ and $|-\rangle$ modes. Increasing the birefringence further (to $\Delta_P/2\pi = 20$ MHz), we find that the cavity emission has flipped and is almost entirely in the $|+\rangle$ mode, which is orthogonal to the polarization originally emitted by the atom. This striking effect can be understood as the adiabatic elimination of $|u^+, 0_+, 1_-\rangle$ in the couplings $|u^-, 0_+, 0_-\rangle \leftrightarrow |u^+, 0_+, 1_-\rangle \leftrightarrow |u^+, 1_+, 0_-\rangle$ (where we have implicitly considered the adiabatic elimination of $|e^0, 0_+, 0_-\rangle$ in the photon production process).

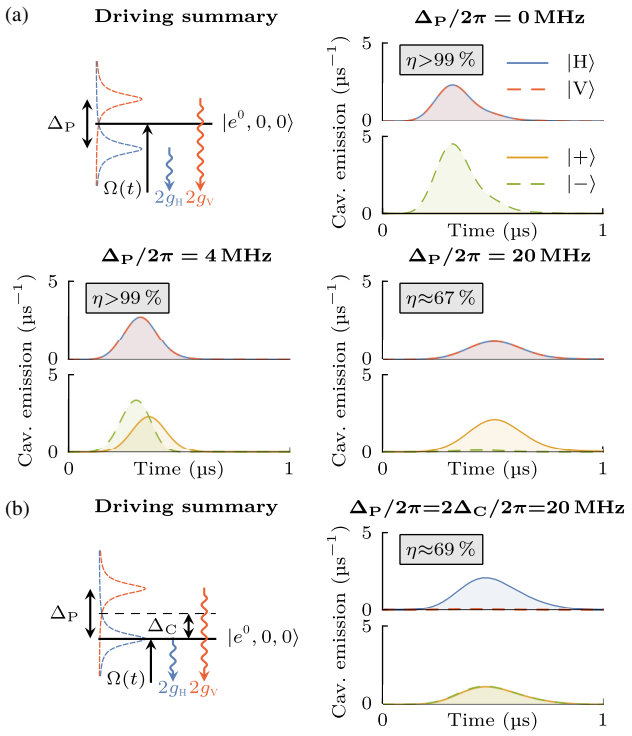

FIG. 4. Polarization dynamics of emitted photons simulated for increasing splitting of the linearly polarized cavity eigenmodes, $|H\rangle$ and $|V\rangle$. Photon emission is driven by a 1 μs pump pulse with a $\sin^4$ intensity profile and a peak Rabi frequency $\Omega/2\pi =$ 7 MHz and $\Omega/2\pi = 2$ MHz for $\Delta_P/2\pi = \{0, 4\}$ MHz and $\Delta_P/2\pi = 20$ MHz, respectively. The cavity resonances are tuned such that either (a) the polarization eigenmodes are oppositely detuned from Raman resonance, or (b) a single polarization eigenmode is on Raman resonance. The photon wave packet is plotted in both a linear and a circular polarization basis, with the overall efficiency of the emission process, η, inset.

The emission efficiency is also reduced by increased birefringence due to the weakened coupling of the atom to the off-Raman-resonant cavity modes. For our system, this necessitates a correspondingly weaker pump pulse; otherwise the dominant effect becomes Rabi oscillations between $|u^-\rangle$ and $|e^0\rangle$. The efficiency is still reduced if one of the cavity eigenmodes is set to be Raman resonant; however for sufficiently large birefringence the cavity emission is then almost entirely into this linear polarization mode [see Fig. 4(b)]. Any cavity, regardless of the splitting or polarization of its eigenmodes, can in principle couple any transition that is not mutually orthogonal to both eigenmodes, as there will always be at least one cavity mode that decomposes to have some contribution of the desired polarization component. In this case, the cavity can then be understood to act as a filter, transmitting only the polarization of light it is capable of supporting. In the paraxial approximation, this precludes π-polarized modes because their field vector points along the cavity axis.

The modified photon polarizations and coupling strengths we have observed have the potential to impact a wide array of cavity-based schemes. For example, in systems where information is encoded into the polarization state of single photons, these effects could lead to a loss of coherence and increased error rates. Additionally, birefringence will result in a distinguishability between different emitter-cavity nodes, even when using inherently homogenous emitters such as atoms or ions. Even supposing that preserving the polarization state of the light is not required, there is still a reduction in coupling strength to any mode not aligned with the cavity eigenmodes.

We foresee the effects and model presented in this Letter as guiding the ongoing efforts towards minimizing and tailoring birefringence in high-cooperativity cavities. This will be essential to future experiments using cavity-enhanced interactions such as the pursuit of scalable quantum network architectures.

The authors would like to acknowledge support for this work through the UK National Quantum Technologies Programme (NQIT hub, EP/M013243/1), and express gratitude for their helpful discussions with A. Beige.

*axel.kuhn@physics.ox.ac.uk

[1] S. Haroche, Rev. Mod. Phys. **85**, 1083 (2013).

[2] M. Brune, E. Hagley, J. Dreyer, X. Maître, A. Maali, C. Wunderlich, J. M. Raimond, and S. Haroche, Phys. Rev. Lett. **77**, 4887 (1996).
[3] S. Gleyzes, S. Kuhr, C. Guerlin, J. Bernu, S. Deléglise, U. Busk Hoff, M. Brune, J.-M. Raimond, and S. Haroche, Nature (London) **446**, 297 (2007).
[4] H. J. Kimble, Nature (London) **453**, 1023 (2008).
[5] C. Monroe, Nature (London) **416**, 238 (2002).
[6] C. Monroe, R. Raussendorf, A. Ruthven, K. R. Brown, P. Maunz, L.-M. Duan, and J. Kim, Phys. Rev. A **89**, 022317 (2014).
[7] A. Reiserer and G. Rempe, Rev. Mod. Phys. **87**, 1379 (2015).
[8] A. Fruchtman and I. Choi, *Technical Roadmap for Fault-Tolerant Quantum Computing* (University of Oxford, Oxford, 2016).
[9] P. B. R. Nisbet-Jones, J. Dilley, D. Ljunggren, and A. Kuhn, New J. Phys. **13**, 103036 (2011).
[10] T. Legero, T. Wilk, M. Hennrich, G. Rempe, and A. Kuhn, Phys. Rev. Lett. **93**, 070503 (2004).
[11] T. Wilk, S. C. Webster, H. P. Specht, G. Rempe, and A. Kuhn, Phys. Rev. Lett. **98**, 063601 (2007).
[12] H. P. Specht, J. Bochmann, M. Mücke, B. Weber, E. Figueroa, D. L. Moehring, and G. Rempe, Nat. Photonics **3**, 469 (2009).
[13] J. McKeever, A. Boca, A. Boozer, R. Miller, J. Buck, A. Kuzmich, and H. Kimble, Science **303**, 1992 (2004).
[14] A. Kuhn, M. Hennrich, and G. Rempe, Phys. Rev. Lett. **89**, 067901 (2002).
[15] G. S. Vasilev, D. Ljunggren, and A. Kuhn, New J. Phys. **12**, 063024 (2010).
[16] P. B. R. Nisbet-Jones, J. Dilley, A. Holleczek, O. Barter, and A. Kuhn, New J. Phys. **15**, 053007 (2013).
[17] M. Keller, B. Lange, K. Hayasaka, W. Lange, and H. Walther, Nature (London) **431**, 1075 (2004).
[18] S. Ritter, C. Nölleke, C. Hahn, A. Reiserer, A. Neuzner, M. Uphoff, M. Mücke, E. Figueroa, J. Bochmann, and G. Rempe, Nature (London) **484**, 195 (2012).
[19] A. Reiserer, N. Kalb, G. Rempe, and S. Ritter, Nature (London) **508**, 237 (2014).
[20] B. Hacker, S. Welte, G. Rempe, and S. Ritter, Nature (London) **536**, 193 (2016).
[21] S. Welte, B. Hacker, S. Daiss, S. Ritter, and G. Rempe, Phys. Rev. X **8**, 011018 (2018).
[22] T. Steinmetz, Y. Colombe, D. Hunger, T. Hänsch, A. Balocchi, R. Warburton, and J. Reichel, Appl. Phys. Lett. **89**, 111110 (2006).
[23] D. Hunger, T. Steinmetz, Y. Colombe, C. Deutsch, T. W. Hänsch, and J. Reichel, New J. Phys. **12**, 065038 (2010).
[24] J. Gallego, S. Ghosh, S. K. Alavi, W. Alt, M. Martinez-Dorantes, D. Meschede, and L. Ratschbacher, Appl. Phys. B **122**, 47 (2016).
[25] J. Gallego, W. Alt, T. Macha, M. Martinez-Dorantes, D. Pandey, and D. Meschede, Phys. Rev. Lett. **121**, 173603 (2018).
[26] M. Steiner, H. M. Meyer, C. Deutsch, J. Reichel, and M. Köhl, Phys. Rev. Lett. **110**, 043003 (2013).
[27] H. Takahashi, E. Kassa, C. Christoforou, and M. Keller, Phys. Rev. A **96**, 023824 (2017).
[28] T. G. Ballance, H. M. Meyer, P. Kobel, K. Ott, J. Reichel, and M. Köhl, Phys. Rev. A **95**, 033812 (2017).
[29] C. Toninelli, Y. Delley, T. Stöferle, A. Renn, S. Götzinger, and V. Sandoghdar, Appl. Phys. Lett. **97**, 021107 (2010).
[30] R. Albrecht, A. Bommer, C. Deutsch, J. Reichel, and C. Becher, Phys. Rev. Lett. **110**, 243602 (2013).
[31] H. Kaupp, T. Hümmer, M. Mader, B. Schlederer, J. Benedikter, P. Haeusser, H.-C. Chang, H. Fedder, T. W. Hänsch, and D. Hunger, Phys. Rev. Applied **6**, 054010 (2016).
[32] A. Muller, E. B. Flagg, M. Metcalfe, J. Lawall, and G. S. Solomon, Appl. Phys. Lett. **95**, 173101 (2009).
[33] J. Miguel-Sánchez, A. Reinhard, E. Togan, T. Volz, A. Imamoglu, B. Besga, J. Reichel, and J. Estève, New J. Phys. **15**, 045002 (2013).
[34] H. Snijders, J. A. Frey, J. Norman, V. P. Post, A. C. Gossard, J. E. Bowers, M. P. van Exter, W. Löffler, and D. Bouwmeester, Phys. Rev. Applied **9**, 031002 (2018).
[35] T. Hümmer, J. Noe, M. S. Hofmann, T. W. Hänsch, A. Högele, and D. Hunger, Nat. Commun. **7**, 12155 (2016).
[36] A. Jeantet, Y. Chassagneux, C. Raynaud, P. Roussignol, J.-S. Lauret, B. Besga, J. Estève, J. Reichel, and C. Voisin, Phys. Rev. Lett. **116**, 247402 (2016).
[37] N. Flowers-Jacobs, S. Hoch, J. Sankey, A. Kashkanova, A. Jayich, C. Deutsch, J. Reichel, and J. Harris, Appl. Phys. Lett. **101**, 221109 (2012).
[38] A. D. Kashkanova, A. B. Shkarin, C. D. Brown, N. E. Flowers-Jacobs, L. Childress, S. W. Hoch, L. Hohmann, K. Ott, J. Reichel, and J. G. E. Harris, Nat. Phys. **13**, 74 (2016).
[39] H. Zhong, G. Fläschner, A. Schwarz, R. Wiesendanger, P. Christoph, T. Wagner, A. Bick, C. Staarmann, B. Abeln, K. Sengstock *et al.*, Rev. Sci. Instrum. **88**, 023115 (2017).
[40] R. Gehr, J. Volz, G. Dubois, T. Steinmetz, Y. Colombe, B. L. Lev, R. Long, J. Esteve, and J. Reichel, Phys. Rev. Lett. **104**, 203602 (2010).
[41] B. Brandstätter, A. McClung, K. Schüppert, B. Casabone, K. Friebe, A. Stute, P. O. Schmidt, C. Deutsch, J. Reichel, R. Blatt *et al.*, Rev. Sci. Instrum. **84**, 123104 (2013).
[42] H. Takahashi, J. Morphew, F. Oručević, A. Noguchi, E. Kassa, and M. Keller, Opt. Express **22**, 31317 (2014).
[43] M. Mader, J. Reichel, T. W. Hänsch, and D. Hunger, Nat. Commun. **6**, 7249 (2015).
[44] S. Garcia, F. Ferri, K. Ott, J. Reichel, and R. Long, Opt. Express **26**, 22249 (2018).
[45] M. Uphoff, M. Brekenfeld, G. Rempe, and S. Ritter, New J. Phys. **17**, 013053 (2015).
[46] T. Wilk, S. C. Webster, A. Kuhn, and G. Rempe, Science **317**, 488 (2007).
[47] H. Huang and K. K. Lehmann, Appl. Opt. **47**, 3817 (2008).
[48] P. Dupré, Phys. Rev. A **92**, 053817 (2015).
[49] A. Ejlli, F. Della Valle, and G. Zavattini, Appl. Phys. B **124**, 22 (2018).
[50] P. Asenbaum and M. Arndt, Opt. Lett. **36**, 3720 (2011).
[51] G. Vasilev, D. Ljunggren, and A. Kuhn, New J. Phys. **12**, 063024 (2010).
[52] T. Wilk, H. P. Specht, S. C. Webster, G. Rempe, and A. Kuhn, J. Mod. Opt. **54**, 1569 (2007).

[53] See Supplemental Material at http://link.aps.org/supplemental/10.1103/PhysRevLett.122.083602, which includes Refs. [54–60], for details of how the Jaynes-Cummings model is extended to consider a birefringent cavity and a characterization of the single-photon source.
[54] A. Kuhn and D. Ljunggren, Contemp. Phys. **51**, 289 (2010).
[55] A. Kuhn, in *Engineering the Atom-Photon Interaction* (Springer, New York, 2015), pp. 3–38.
[56] J. Johansson, P. Nation, and F. Nori, Comput. Phys. Commun. **184**, 1234 (2013).
[57] C. A. Brasil, F. F. Fanchini, and R. de Jesus Napolitano, Rev. Bras. Ensino Fis. **35**, 01 (2013).
[58] P. Pearle, Eur. Phys. J. **33**, 805 (2012).
[59] C. K. Hong, Z. Y. Ou, and L. Mandel, Phys. Rev. Lett. **59**, 2044 (1987).
[60] T. Legero, T. Wilk, A. Kuhn, and G. Rempe, Adv. At. Mol. Opt. Phys. **53**, 253 (2006).
[61] H. J. Kimble, Phys. Scr. **T76**, 127 (1998).
[62] L. Sánchez-Soto, J. Monzón, and G. Leuchs, Eur. J. Phys. **37**, 064001 (2016).
[63] This barred notation indicates that the angular dependence of each transition has not been included, which we consider explicitly due to the asymmetrically shifted coupling strengths in our system that are a result of the non-negligible magnetic field (as detailed in Ref. [64]). For example, the Rabi frequency of the $|F=1,m_F=\pm1\rangle \leftrightarrow |F'=1,m'_F=0\rangle$ couplings in zero magnetic field is $\sqrt{5/24}\times\bar{\Omega}$, with the appropriate prefactor for different transitions readily available in standard reference books [65]. The quoted atom-cavity coupling rate, $g/2\pi = 4.77$ MHz, similarly assumes the zero-field transition strengths. The laser-cavity Raman resonance was experimentally optimized to $2\pi\times$ 7.5 MHz above the zero field $|F=1,m_F=0\rangle$ to $|F'=1,m'_F=0\rangle$ transition frequency as necessitated by the nonlinear Zeeman effects [64].
[64] T. D. Barrett, D. Stuart, O. Barter, and A. Kuhn, New J. Phys. **20**, 073030 (2018).
[65] D. A. Steck, Rubidium 87D Line Data, http://steck.us/alkalidata/rubidium87numbers.pdf.
[66] Photon Spot, Model No. NW1FC780.
[67] Qutools quTAU.
[68] The reduced chi-squared parameters [69] for the theoretical fits to the measured data for σ^- emission in Fig. 2(c) are $\chi^2_\nu = 1.1$ ($\chi^2_\nu = 11.0$) for $|H\rangle$ and $\chi^2_\nu = 2.3$ ($\chi^2_\nu = 23.7$) for $|V\rangle$ for the fits including (excluding) cavity birefringence effects. An equivalent analysis for σ^+ emission from the atom gives $\chi^2_\nu = 5.7$ ($\chi^2_\nu = 14.4$) for $|H\rangle$ and $\chi^2_\nu = 8.4$ ($\chi^2_\nu = 18.0$) for $|V\rangle$. Systematic effects due to optical elements beyond the cavity were verified to be negligible with the polarization of light passing through both vacuum chamber viewports rotated by $< 1.3\%$. The purity of the photon polarization states exceeds the best observed routing of 91% (achieved at $\phi = -68.5°$ for σ^- emission), as this is averaged over the entire length of the time-dependent photon states and achieved with only a quarter-wave plate.
[69] I. Hughes and T. Hase, *Measurements and Their Uncertainties: A Practical Guide to Modern Error Analysis* (Oxford University Press, Oxford, 2010).

Correction: The previously published Figure 4 contained an error in the units and has been replaced.